

Imaging and Automated Detection of *Sitophilus oryzae* (Coleoptera: Curculionidae) Pupae in Hard Red Winter Wheat

MICHAEL D. TOEWS, TOM C. PEARSON, AND JAMES F. CAMPBELL

USDA-ARS Grain Marketing and Production Research Center, 1515 College Avenue, Manhattan, KS

J. Econ. Entomol. 99(2): 583-592 (2006)

ABSTRACT Computed tomography, an imaging technique commonly used for diagnosing internal human health ailments, uses multiple x-rays and sophisticated software to recreate a cross-sectional representation of a subject. The use of this technique to image hard red winter wheat, *Triticum aestivum* L., samples infested with pupae of *Sitophilus oryzae* (L.) was investigated. A software program was developed to rapidly recognize and quantify the infested kernels. Samples were imaged in a 7.6-cm (o.d.) plastic tube containing 0, 50, or 100 infested kernels per kg of wheat. Interkernel spaces were filled with corn oil so as to increase the contrast between voids inside kernels and voids among kernels. Automated image processing, using a custom C language software program, was conducted separately on each 100 g portion of the prepared samples. The average detection accuracy in the five infested kernels per 100-g samples was $94.4 \pm 7.3\%$ (mean \pm SD, $n = 10$), whereas the average detection accuracy in the 10 infested kernels per 100-g sample was $87.3 \pm 7.9\%$ ($n = 10$). Detection accuracy in the 10 infested kernels per 100-g samples was slightly less than the five infested kernels per 100-g samples because of some infested kernels overlapping with each other or air bubbles in the oil. A mean of 1.2 ± 0.9 ($n = 10$) bubbles (per tube) was incorrectly classed as infested kernels in replicates containing no infested kernels. In light of these positive results, future studies should be conducted using additional grains, insect species, and life stages.

KEY WORDS insect-damaged kernels, stored-product insects, sampling, internal infestation, computed tomography

Insect-damaged kernels (IDK) result when an internal infesting species completes development in a kernel of grain and then the adult bores its way out leaving an emergence hole. *Rhyzopertha dominica* (F.) (Coleoptera: Bostrichidae), *Sitophilus granarius* (L.) (Coleoptera: Curculionidae), *Sitophilus oryzae* (L.), *Sitophilus zeamais* Motschulsky, and *Sitotroga cerealella* (Olivier) (Lepidoptera: Gelechiidae) are responsible for internal infestations of U.S. stored wheat, *Triticum aestivum* L. These species consume large quantities of grain and are generally regarded as the most damaging of stored-wheat insects (Pedersen 1992). Storey et al. (1982) studied wheat at U.S. terminals and found a four-fold increase in grain infestation rates when the samples were incubated to detect internal infestations. IDK are quantified as part of the formal grain grading procedures defined in the Official United States Standards for Grain (GIPSA 1993), and samples containing >31 IDK per 100 g are classified as sample grade-wheat unfit for human consumption. Domestic flour mills generally specify they

will not accept wheat with >5 IDK per 100 g or any live insects (Bob Richardson, personal communication).

Rapid detection of hidden insect infestations is important to both the grain storage and milling industries. Managers storing wheat could use information about hidden infestation as a means of assessing the potential for future infestation, for example, a single *S. oryzae* female can lay up to 384 eggs (Birch 1945). Insect feeding can be an indicator that the grain is out of condition or more susceptible to mold and fungal infection. Internally infested kernels may contaminate processed foods with metabolic waste products and contribute to the number of insect fragments in finished flour. Insect fragments in flour are regulated by a defect action level of <75 fragments per 50 g (FDA 1988).

There are no rapid methods of quantifying internally infested kernels in large quantities of grain. Currently accepted procedures, although notoriously slow, include x-ray examination (American Association of Cereal Chemists [AACC] method 28-21) and the crack and float method (AACC methods 28-22 and 28-51) (AACC 1995). Methods such as egg plug staining techniques (Goosens 1949) and placing kernels in a solution with a specific gravity that will allow sound

Mention of trade names or commercial products in this publication is solely for the purpose of providing specific information and does not imply recommendation or endorsement by the U.S. Department of Agriculture.

kernels to sink, whereas infested kernels float (White 1957), present practicality constraints for large samples. Dennis and Decker (1962) developed a method to detect free amino acids released when infested kernels were crushed with ninhydrin-treated paper, whereas other studies (Wehling and Wetzler 1983, Wehling et al. 1984) detected an insect-excreted by-product, uric acid, by using chromatography. Myosin, an insect muscle protein (Quinn et al. 1992), can be detected using an enzyme-linked immunosorbent assay that is commercially available (Schatzki et al. 1993, Brader et al. 2002). However, it is difficult to quantify the number of infested kernels with these methods. Pearson et al. (2003) developed algorithms to detect internal infestations in wheat based on 300 kernel samples passed through the Perten Single Kernel Characterization System (SKCS), whereas others (Ridgway and Chambers 1996, Dowell et al. 1998) investigated using near-infrared reflectance (NIR) spectroscopy to determine differences in absorption because of the presence of internal infestations. The most recent published work used real-time x-ray inspection and automated detection software (Karunakaran et al. 2003a, b, Karunakaran et al. 2004, Haff and Slaughter 2004).

Computed tomography scanners use x-ray technology and sophisticated software to recreate cross-sectional displays of the subject. These scanners are commonly used in medical facilities for diagnosing human medical conditions. Data are collected in thin "slices" or frames that can be viewed in the same sequence they were scanned. The resulting display represents the x-ray absorption of the material being scanned, which is a function of density and chemical composition of the material (Mohsenin 1984). In general, more dense materials (e.g., grain) permit less radiation to pass, resulting in lighter exposed areas on the display, whereas less dense materials (e.g., voids in kernels caused by insects) permit more radiation to pass and result in darker areas on the display. Previous entomological applications of computed tomography include studying the burrowing of pecan weevils (Harrison et al. 1993) and tracking insect movement within soil (Johnson et al. 2004).

The research approach taken here was fundamentally different than that of other studies in the literature. Previous studies (Karunakaran et al. 2003a, 2004; Haff and Slaughter 2004) examined 1,074–1,500 total kernels of which approximately one-half (600) were infested. Because industry is only interested in receiving grain with <6 IDK per 100 g, we took the approach that any new method will require the ability to discern infested kernels at extremely low densities with virtually no false positives. Here, we examined $\approx 90,000$ kernels of which 150 were infested. To examine ≈ 600 infested kernels at a realistic infestation density would require scanning ≈ 12 kg of grain (36 scans), which was not feasible. The objectives of the study were to 1) refine sample preparation methodologies to maximize the contrast between *S. oryzae*-infested and uninfested hard red winter wheat samples when imaged using computed tomography, 2) determine

issues involved in accurate detection of insects by using 100-g samples infested at densities near action thresholds, and 3) develop software to rapidly recognize and quantify infested kernels in 100-g wheat samples.

Materials and Methods

Insect Cultures. *S. oryzae* was reared in the laboratory in 0.9-liter glass jars containing 300 g of hard red winter wheat equilibrated to 13.5% moisture content. The founding colony was collected in eastern Kansas before 1960. The colony was maintained in the laboratory at $28.0 \pm 0.5^\circ\text{C}$ and $60 \pm 5\%$ RH in environmental growth chambers with a photoperiod of 12:12 (L:D) h. Rearing density was ≈ 100 adults per 300 g of wheat.

Pupae used in experiments were obtained by placing ≈ 300 adults (<1 wk old) on 100 g of wheat for a 24-h oviposition period. Immatures developed for 23 d and then infested kernels were selected using x-ray analyses (Throne 1994). Kernels were laid crease down in a monolayer on top of previously exposed radiograph film that was placed on top of a new film packet (Industrex MX125, Eastman Kodak, Rochester, NY). The film was exposed to an x-ray source (model 43855A, Faxitron X-ray Corp., Wheeling, IL) at 18 kV and 3 mA for a duration of 3 min. Radiographs were then examined under a $10\times$ dissecting microscope with a darkfield base (SMZ1000, Nikon Instruments Inc., Melville, NY). Kernels containing pupae were immediately frozen for 24 h at -22°C to kill the insects. Infested kernels were radiographed a second time for quality control purposes.

Wheat. Hard red winter wheat used in all experiments was procured directly from the field in May 2002 from a grower in Dickinson County, Kansas, who used standard agronomic practices. Wheat was passed over an electric dockage tester (Carter Day International, Minneapolis, MN) a minimum of six times to remove all dockage, foreign material, and broken kernels. After cleaning, wheat was probed using a grain trier (No. 20-OH, Seedburo Equipment Co., Chicago, IL), and the resulting grain samples were radiographed as described above to inspect for residual insect infestation. No signs of internal insect infestation were observed, and the wheat was stored in a sealed container located in a cold room (10°C) until use in experiments.

Computed Tomography Imaging. Imaging was conducted on a high-speed spiral computed tomography scanner (model Mx 8000, Royal Philips Electronics, Best, The Netherlands). Parameters selected for each scan were 140 kV and 96 mA. High-resolution cross-sectional slices, each 0.6 mm in thickness, were obtained 0.3 mm apart, resulting in a 50% overlap between adjacent slices. The scanner interpolated each frame into a 512 by 512 pixel matrix, resulting in a resolution of 3.42 pixels per mm. Individual jars or tubes of grain were scanned with the container horizontally on its side and scans progressed toward the top of the jar.

Optimization of Contrast Enhancement. Studies were initiated to refine sample preparations that would provide the maximum contrast between infested kernels and voids among kernels. Uninfested wheat was placed in a 300-ml (65-mm-o.d.) high-density polyethylene jar (model 1101471500, Pretium Packaging, St. Louis, MO) that held 240 g of wheat. The jar was filled approximately half full with uninfested wheat, and then three infested kernels were manually placed in the jar, orientated so that they did not touch each other. Uninfested wheat was then added until the jar was full. The jar and its contents were scanned using the computed tomography scanner, and images were saved as audio video interleave (AVI) files (Microsoft, Redmond, WA).

A variety of liquid and dry materials were used to try and fill the interkernel spaces and thereby increase contrast between the insect tunnels in infested kernels and spaces among kernels. A single scan (≈ 150 g of wheat per scan) was conducted with each filler including diatomaceous earth (INSECTO, Natural INSECTO Products, Inc., Costa Mesa, CA), distilled water, corn oil (Mazola, ACH Food Co. Inc., Memphis, TN), paint thinner (GPT1K, W.M. Barr & Co., Inc., Memphis, TN), red gauge oil (Dwyer Instruments Inc., MI City, IN), and wheat flour (short patent flour, Stafford County Flour Mills Co., Hudson, KS). After first filling the jar with wheat and infested kernels as described above, liquid fillers were added until the liquid reached the top of the jar. Diatomaceous earth or wheat flour were manually mixed with the wheat at a rate of 5:1 (wheat:filler) and then poured into the jar.

Qualitative and quantitative analyses were conducted on the images derived from each scan. Individual bit-mapped graphics format (BMP) images were extracted from the AVI video files by using a commercial program (Zilla Video Converter-Decompiler version 1.40, ZillaSoft LLC, Taunton, MA). While viewing each frame in sequence, infested kernels were located, and the contrast between those kernels and the surrounding media was visually assessed.

Depending on the liquid filler tested, air bubbles of varying quantity and size occurred. Because air bubbles could easily be confused with infested kernels, a protocol was developed using portions of the scans containing no infested kernels to estimate the number of air bubbles in each treatment as a means of evaluating potential filler suitability. By treatment ($n = 4$ per treatment), contiguous groups of 28 frames each (each group representing ≈ 25 g wheat) were combined to make image stacks by using an image analysis program (ImageJ version 1.30, Nation Institutes of Health, Bethesda, MD). Because shading intensity in the image is a relative measure of density, the standard deviation of each transverse string of pixels was calculated through all 28 frames contained in the group. In theory, the standard deviation of a group of pixels through sound kernels and liquid would be small; however, presence of an air bubble would increase the pixel standard deviation because bubbles have no density. The resulting stacked frame images (Fig. 1) were

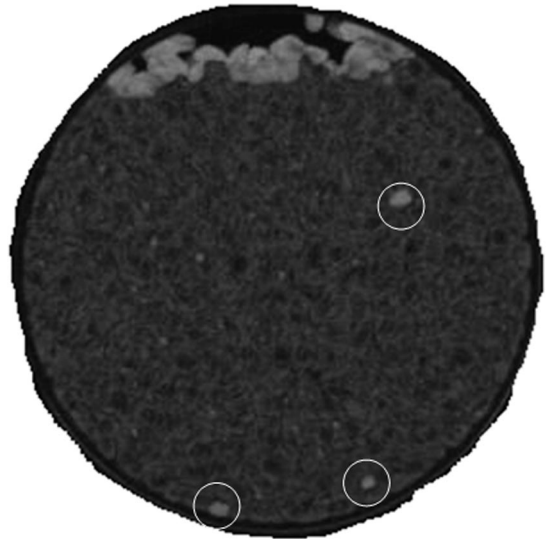


Fig. 1. Display of a 28-frame stacked group with three air bubbles circled. Not enough liquid was added to completely fill the container resulting in the lighter areas at the top of the display.

interpreted by enumerating the light areas (air bubbles), which contrasted with the dark matrix.

Quantification of Infested Kernels. This experiment was conducted to examine larger samples of grain and develop a rapid means of quantifying the number of infested kernels. Three 1-kg batches of uninfested grain were weighed on a microbalance (model E1RW60, Ohaus Corp., Florham Park, NJ). One batch contained no infested kernels (control). For the second batch, 50 sound kernels were replaced with 50 infested kernels; likewise, 100 sound kernels were replaced with 100 infested kernels in the third batch. These sample densities correspond to 0, 5, or 10 infested kernels per 100 g of wheat. The second and third samples were individually mixed in a Mac Lellan batch mixer (Anglo American Mill Corp., Inc., Owensboro, KY) for 10 min to randomize the location of the infested kernels within each sample.

The vessel for grain imaging was prepared as follows. An acrylic disk was glued to one end of a 91-cm-long clear cast acrylic hollow rod (76.2 mm o.d. by 69.9 mm i.d.) by using minute-bond adhesive. Fifty grams of uninfested wheat was placed in the tube, and the top of the grain surface was marked by adhering a topographic marker (#462-013, Radiation Products Design, Inc., Albertville, MN) to the outside of the tube. The previously prepared sample was then added and the top of the grain surface was marked with a second topographic marker. Finally, another kilogram of uninfested wheat and enough corn oil (≈ 1 liter) to rise above the top of the wheat were added. It was hypothesized that increasing the depth of the prepared sample in the corn oil would allow air bubbles to rise upward and out of the zone of the prepared sample. The top end of the hollow rod was capped with a 27.9-cm rubber balloon inflated through a 4.1-

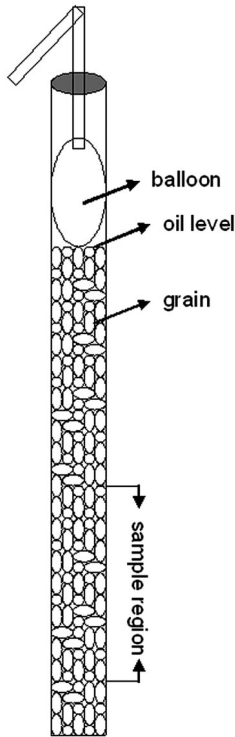


Fig. 2. Sample vessel prepared for imaging on the computed tomography scanner. Sample region is ≈ 30 cm in length.

cm-o.d. hollow tube. At the opposite end of the hollow tube was a short piece of 9.5-mm-o.d. rubber tubing that could be bent over and clamped using a Rankin forceps after balloon inflation (Fig. 2). Samples were scanned 1 cm beyond each of the topographic markers to ensure the entire prepared sample was imaged.

Image Processing. BMP format images were extracted from all frames of the AVI video files. Each individual frame was viewed in sequence while manually enumerating air bubbles or infested kernels; additionally, orientation of kernels containing insect tunnels was noted. These kernels were classified as either side-oriented (presented with the kernel lying on a side, crease up, or crease down) or axially oriented (presented cross-sectional, brush to germ, or vice versa). More complex methods of separating air bubbles from infested kernels were investigated with this raw data set.

Each 1-kg prepared sample comprised $\approx 1,050$ frames. For descriptive purposes, each point in the sample was represented by $u(x, y, z)$, where x and y are the coordinates of each pixel, and z is the frame number (from 1 to 1,050). For all z between 10 and 1,050, a composite image $u_{min}(x, y, z)$ was created by taking the minimum pixel intensity at each x and y location for 10 images in the interval from $z-10$ to z . Next, for all z , each $u_{min}(x, y, z)$ was thresholded such that if $u_{min}(x, y, z) < 20$, then $u_{min-threshold}(x, y, z) = 1$, otherwise $u_{min-threshold}(x, y, z) = 0$. Thus, each z , $u_{min-threshold}(x, y, z)$ likely contained voids indicating the presence of either air bubbles or infested kernels.

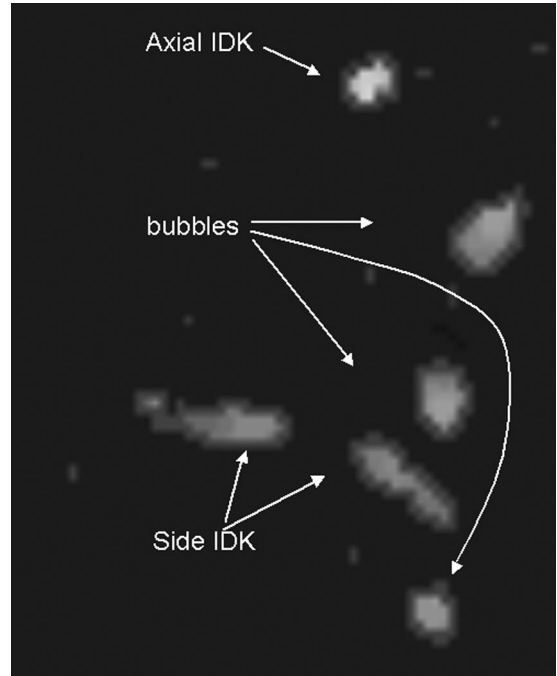


Fig. 3. Portion of a composited and thresholded image containing two side-oriented infested kernels, one axially oriented infested kernel, and three air bubbles.

All $u_{min-threshold}(x, y, z)$ were divided into 10 equal sections comprising $z = 105$ images. As shown in the equation below, each section of 105 frames was integrated into a single frame to scrutinize differences in void size, shape, and density:

$$I_j(x, y) = \sum_{z=j^{*}105+1}^{j^{*}105+105} u_{min-threshold}(x, y, z)$$

for $j = 0, 1, \dots, 9$

This processing was performed in a custom written C language program. Each $I_j(x, y)$ can be thought of as a contour plot of all infested kernels and bubbles found in ≈ 100 -g samples of wheat. A portion of one $I_j(x, y)$ is shown in Fig. 3.

Based on preliminary analyses of the composite images, size characteristics in a two-dimensional plane were used to separate air bubbles from insect-infested kernels. The length, width, void area, and maximum pixel intensity for each void in all $I_j(x, y)$ were computed using an image analysis program (ImageJ version 1.31, National Institutes of Health). Because most air bubbles in the size range of insect tunnels were round in shape, side-oriented infested kernels could be distinguished from the air bubbles by the length-to-width ratio. Insect tunnels in axially oriented kernels also had a round shape, but they generally had brighter pixel intensity than air bubbles. The longer length of the insect tunnel resulted in higher values when $I_j(x, y)$ was computed, which translated into

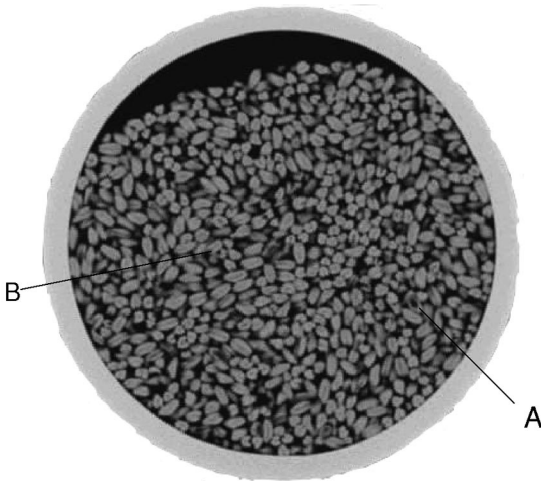


Fig. 4. Example frame of wheat scanned with no filler material. (A) Presence of an insect tunnel. (B) Presence of a false positive occurring because of the axial-oriented kernel.

brighter pixel intensity. Insect-infested kernels always had void areas between 20 and 120 pixels; therefore, voids outside this range were automatically classified as air bubbles.

Normal linear regression was used to illustrate the relationship between all counts derived from the computer program and the known number of actual infested kernels, and 95% inverse prediction confidence limits (Neter et al. 1996) were calculated for that regression equation. The regression equation can be used as a calibration curve to estimate the actual number of infested kernels in a new grain sample, based on the number of infested kernels identified by the software program described above, and the inverse regression puts confidence limits on that estimate. In short, the calibration curve will allow the experimenter to use computer generated counts (a quick, approximate measurement) to estimate number of infested kernels (a precise, time-consuming measurement) with 95% confidence.

Results

Optimization of Contrast Enhancement. The first computed tomography scan of wheat showed potential for a new means of hidden insect detection, but there are hurdles that must be overcome. First, the orientation of the kernels in the grain mass made a difference as to the appearance of infested versus uninfested kernels (Fig. 4). Uninfested kernels that were side oriented seemed intact. Axially oriented kernels, although few in number, seemed to have a small void through the center. Insect-infested kernels had a much larger void that consumed the majority of the kernel volume regardless of kernel orientation.

In-depth analyses of samples prepared using dry filler materials proved problematic. Diatomaceous earth has a low density, so it permitted too much x-ray

Table 1. Mean \pm SD, minimum, and maximum bubble counts in groups of 28 frames (\approx 25 g of wheat) when interkernel spaces were filled with liquid fillers

Filler material	Mean ^a \pm SD	Min	Max
Distilled water	160.5 \pm 15.5	143	174
Corn oil	25.0 \pm 27.2	0	51
Paint thinner	35.0 \pm 11.7	20	48
Red gage oil	84.3 \pm 8.6	75	92

^a $n = 4$.

radiation to pass, resulting in similar contrast problems as described above when using no filler material. Wheat flour did not evenly distribute throughout the sample, resulting in a similar problem in some areas. As a result of these difficulties, further consideration was reserved for liquid fillers only.

There were obvious qualitative differences in the scans made with different liquid filler materials. Air bubble quantity among kernels was 6 times greater when water was used as a filler material compared with corn oil (Table 1). The quantity of air bubbles was greater near the top of the sample jars compared with near the bottom; this likely occurred because bubbles rose to the top when jars were placed with the lid up in preparation for scanning. In addition to the presence of air bubbles, contrast between interkernel voids and voids in insect-infested kernels varied significantly (Fig. 5). Corn oil was selected for future investigation in subsequent work.

Relatively little time was required to prepare and scan the samples. After the jar was filled with grain, it took \approx 40 s for the corn oil to completely diffuse to the bottom of the jar, whereas less viscous materials (distilled water and paint thinner) took only a few seconds. Computed tomography scans required $<$ 30 s to scan 150 g of wheat.

Quantification of Infested Kernels. From the 30 $I_j(x, y)$ images (each image representing \approx 100 g of grain), 297 voids in total were present that fit the size range between 20 and 120 pixels. Of these voids, 150 were attributed to prepared infested kernels, leaving 147 voids caused by air bubbles. The data were divided into two subsets based on the number of pixels in the void: voids with $<$ 60 pixels were more likely to be axially oriented insect tunnels, whereas voids with $>$ 60 pixels were more likely to be side-oriented insect tunnels (Table 2).

The software program classified voids based on observed frequencies of discrete void sizes, shapes, and pixel intensities. Each subgroup of voids had unique distributions of length-to-width ratios and maximum pixel intensities that were fit with a normal curve (Figs. 6 and 7). The point where the normal curves intersected was set as a threshold value to classify a void as either an air bubble or insect tunnel. Large voids with a length-to-width ratio \leq 1.68 were classified as bubbles, whereas voids with larger length-to-width ratios were classified as infested kernels. This procedure alone correctly classified 87.3% of the known infested kernels and 76.7% of the air bubbles. Small voids with maximum pixel intensities \leq 18

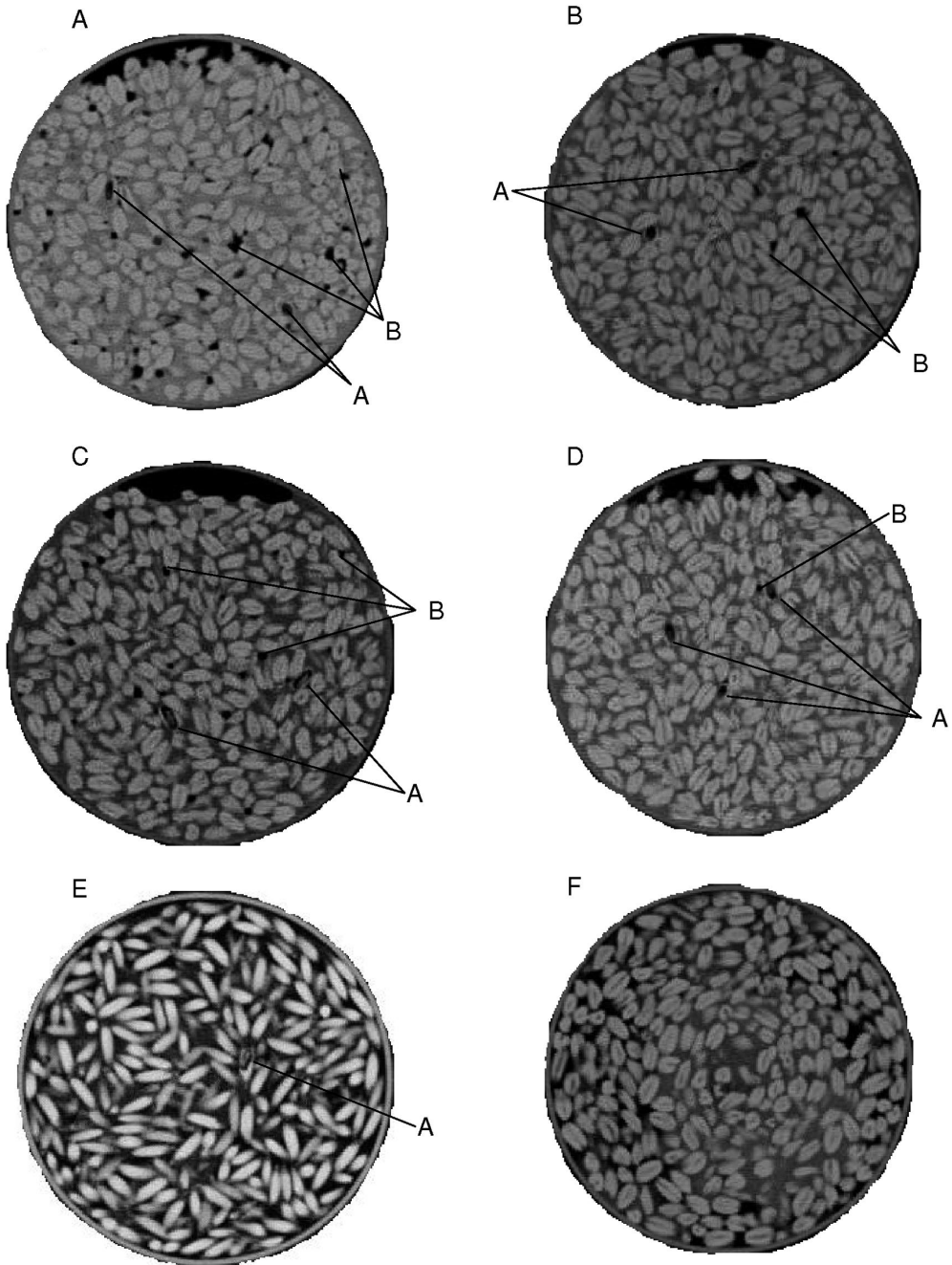


Fig. 5. Example frames of wheat scanned with different filler materials, including distilled water (A), paint thinner (B), red gauge oil (C), corn oil (D), diatomaceous earth (E), and wheat flour (F). (A) Presence of an insect tunnel. (B) Presence of air bubbles. There are no infested kernels depicted in F.

were classified as air bubbles, whereas all other voids were classified as insect tunnels. This procedure correctly classified 91.7% of the insect tunnels that were axially oriented and 84.1% of the small air bubbles. Expected classification error rates on all data using the fitted normal curves were similar to those actually recorded. These accuracies are 92.1% for axially ori-

ented infested kernels, 88.1% for side-oriented infested kernels, 84.1% for small air bubbles, and 83.2% for large air bubbles.

In the 30 $I_j(x, y)$ (composite) images, the number of infested kernels was variable, ranging from 6 to 21 in the 10 infested kernel per 100-g samples ($n = 10$) and from 1 to 8 in the five infested kernels per 100-g

Table 2. Mean \pm SD pixel count, maximum pixel intensity, and length-to-width ratio of voids containing between 20 and 120 pixels

Void type	<i>n</i>	Pixel count	Max pixel intensity	Length-to-width ratio
Bubbles with <60 pixels	57	36.1 \pm 10.5	15.8 \pm 2.3	1.3 \pm 0.3
Bubbles with >60 pixels	90	82.7 \pm 12.4	15.3 \pm 1.7	1.5 \pm 0.3
Axial-oriented infested kernels	24	47.1 \pm 9.3	21.7 \pm 2.3	1.3 \pm 0.1
Side-oriented infested kernels	126	90.0 \pm 11.8	15.7 \pm 1.4	2.0 \pm 0.3

samples ($n = 10$). Detection of infested kernels by the computer program in the five infested kernels per 100-g samples was $94.4\% \pm 7.3\%$ (mean \pm SD). Similarly, detection accuracy by the program in the 10 infested kernels per 100-g sample was $87.3 \pm 7.9\%$. Detection accuracy decreased in the 10 infested kernels per 100-g samples compared with the five infested kernels per 100-g samples because more infested kernels per sample increased the probability that they overlapped with each other or air bubbles in the composite image. In the treatment containing no infested kernels, an average of 1.2 ± 0.9 ($n = 10$) bubbles was incorrectly classified as infested kernels by the computer program. Thus, with 99% confidence, no single uninfested 100-g sample should have a bubble count of more than three.

The actual infested kernel counts versus the counts derived from the imaging program by using the described procedure were very similar. The scatter plot and normal regression (Fig. 8) show a strong relationship when the computer counts were regressed on the known number of insect-infested kernels ($F = 875.3$; $df = 1, 28$; $P < 0.01$). Results presented from the computer program include all voids classed as infested kernels, so this count includes some bubbles incorrectly classified as infested kernels. Inverse prediction 95% CL show the expected variation when using computer counts to estimate the number of infested kernels. For example, if the computer program indicates that the sample contains 10 infested kernels, the actual

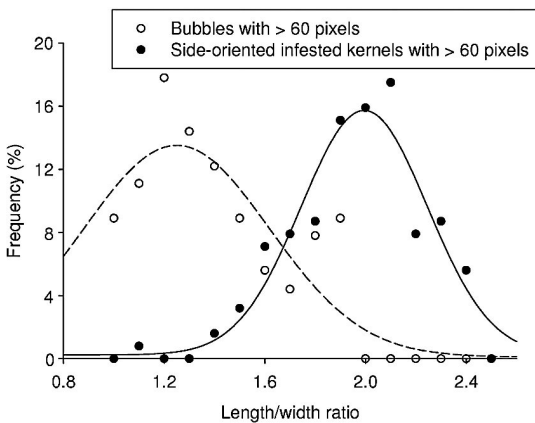


Fig. 6. Distribution of length-to-width ratios and fitted normal curves for insect tunnels and air bubbles containing between 20 and 60 pixels.

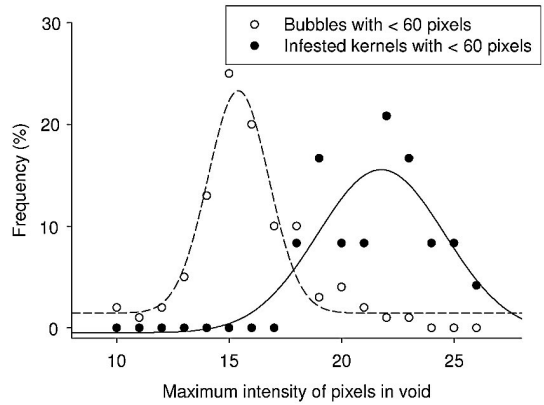


Fig. 7. Distribution of maximum pixel intensities and fitted normal curves for insect tunnels and air bubbles containing between 60 and 120 pixels.

number of infested kernels would fall between 8.3 and 12.3. This amount of error indicates that up to three computer counts could be tolerated in a single 100-g sample and still fall under the five or fewer infested kernel threshold.

Time requirements for preparation and imaging were greater than required for the 150-g scans. It required ≈ 15 min to diffuse all of the corn oil to the bottom of the sample vessel. At one point the oil in the tube was left for an extended period (overnight), but this produced many more bubbles, probably a result of grain respiration. Imaging the entire kilogram prepared sample at once was problematic because it overheated the x-ray tube on the computed tomography scanner and required intermittent cooling. In general, ≈ 400 g of grain could be scanned in 1.5 min. The cooling period varied from 3 to 5 min, depending on how much the scanner was used before these scans.

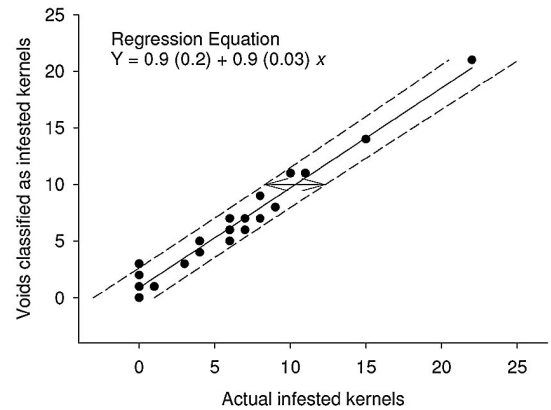


Fig. 8. Scatter plot of actual infested kernel counts and voids classified as infested kernels by our software program for each 100-g sample. The solid line is the linear regression, whereas the dashed lines are the 95% inverse prediction confidence limits. Arrows denote the point estimated confidence limits around $x = y = 10$.

Discussion

The principal advantage to using computed tomography for internal insect detection is the speed at which grain samples were scanned and the number of infested kernels quantified. A representative portion (100–400 g) of a 1-kg sample submitted for grading could be scanned in 1 to 2 min. Other studies have achieved good detection accuracy but lack the ability to inspect large quantities of grain rapidly. For example, Pearson et al. (2003) showed excellent automated insect detection results with the SKCS, but the results are based on a 300-kernel sample (≈ 10.5 g) that required ≈ 2.5 min to scan. Ridgway and Chambers (1996) established a well defined NIR spectroscopy response in wheat infested with *S. granarius*, but the process lacked good sensitivity when tested with bulk samples. Similarly, Dowell et al. (1998) had good results with NIR spectroscopy to detect insect infestations in single kernels at a rate of one kernel per 4 s. Chambers et al. (1984) showed that nuclear magnetic resonance spectroscopy could detect 10 infested kernels in a 500-kernel mass in only 8 s, but additional studies were not conducted.

Admittedly, only one true replication was conducted with each of the filler materials tested. However, our objective was to identify sample preparation methodologies that showed the most promise for further study, and the results suggested that additional work with dry fillers and most of the liquid fillers would not be particularly fruitful. There were actually two candidate fillers that may work well for future studies. Paint thinner performed similar to corn oil in our tests, but corn oil was the best candidate for additional testing because it was more economical and had fewer exposure or disposal hazards associated with its use. Dry fillers generally did not work well because of even distribution problems. Additional procedures, such as tapping the sample jar while loading or using an industrial vibrator, were investigated with little success. Getting smaller dry particulates to move in equal proportion with the larger wheat kernels is also a problem when filling grain bins because the fines tend to stay in the center of the bin and do not move outside of the spoutline (Toews and Subramanyam 2002).

False positives, sound kernels or bubbles classified as infested kernels, were usually caused by air bubbles. Bubbles presented the biggest challenge to automating the detection process, and novel methods for preventing or eliminating air bubbles need to be researched. In preliminary trials, dirty wheat caused many more air bubbles than cleaned wheat. Perhaps better cleaning than passing the grain over a mechanical dockage tester would improve the situation. Adjuvant surfactants or slightly heating the oil to decrease viscosity may be suitable means of decreasing air bubbles and would have the additional benefit of decreasing the time needed for sample preparation. Similar food oils like vegetable, sunflower, or canola may be good candidates for additional investigation.

Some infested kernels in the 10 infested kernels per 100-g samples were underreported because they overlapped with other infested kernels in the composite images. However, detection accuracy at the realistic infestation levels is more important than accuracy at levels >5 infested kernels per 100 g because these loads would likely be rejected and therefore not milled. Accuracy of enumerating infested kernels actually increased at lower infestation densities by using methods described here. Accuracy and prediction confidence intervals, based on 10 replications, show a method with workable accuracy at industry accepted infestation densities.

Adoption of any technology that provides detection of infested kernels will require research-based thresholds about how many infested kernels can be tolerated in the incoming millstream are needed. There is little or no correlation between insect-damaged kernels and the degree of internal insect infestation (Perez-Mendoza et al. 2004); therefore, the de facto economic threshold (5 IDK per 100-g sample) is unreliable for predicting internal infestation. Perez-Mendoza et al. (2005) milled hard red winter wheat samples containing known numbers of *R. dominica*-infested kernels; they showed that the maximum allowable infestation levels to maintain counts below 75 fragments per 50-g flour threshold were 500 larvae, 300 pupae, or 20 newly eclosed adults, respectively.

Computed tomography is different than traditional x-ray radiography because the kernels do not have to be exposed in a monolayer and thus much larger samples can be imaged at one time. Real-time x-ray imaging allows the subject to be exposed and captured in as little as a few milliseconds, but the analyses have not developed to the point where a bulk sample can be analyzed. Karunakaran et al. (2003a, 2004) imaged individual wheat kernels and then successfully used parametric and nonparametric classifiers to quantify the infested kernels. This procedure has been used to identify $>95\%$ of uninfested kernels and kernels infested by larval stages, whereas $>99\%$ of kernels with pupae and adults were identified. Although manual placement of individual kernels for imaging is tedious, it could be accelerated with a grain kernel singulation device (Melvin et al. 2003). A second approach (Haff and Slaughter 2004) is to image many kernels (≈ 350) in a monolayer at one time and then crop them into single kernel images before analyses. Although these methods are slower, image resolution in a monolayer will always be better than in a three-dimensional grain mass. Because axial-oriented wheat kernels seemed to have a small tunnel in them, this will likely be a limiting factor to detect young larvae. Real-time x-ray systems will undoubtedly be able to detect younger life stages than the computed tomography method, but the tunnel also shows up with real-time x-ray imaging if the kernels are axially oriented during exposure. For practical purposes, the resolution of the computed tomography method need only be good enough to find kernel voids as opposed to visible insects.

Cost of a computed tomography scan is an obvious concern for commercial viability of the techniques

described above. Modern computed tomography scanners housed in medical facilities are constructed with the versatility to scan everything from delicate nasal tissues to abdominal cross sections of obese patients. However, all of the scans described here were conducted using identical parameters. We suggest that new equipment using computed tomography principles could be developed that meets the needs of large grain inspection facilities while balancing the economic costs. Because medical facilities constantly update their equipment to get better resolution or scanning speed, there is potential to use outdated medical equipment or some portion of it to create basic computed tomography scanners that meet the more limited resolution requirements for grain inspection.

Additional studies are needed to elucidate the ability of the computed tomography method to detect additional life stages and species. We hypothesize that larger larvae, pupae, and adults will not be a problem regardless of species, and the technique should work equally well with other cereal grains and dry beans.

Acknowledgments

We thank Jackie Rowan and Matt Kennedy for excellent technical support. Mercy Imaging, LLC (Manhattan, KS) and Jason McKinsey graciously donated time and expertise that made this project possible. We thank Noel White and Ron Haff for critically reviewing an earlier manuscript draft. This work was funded with partial support from USDA-CSREES (RAMP) under Agreement No. 00-511-01-9674.

References Cited

- [AACC] American Association of Cereal Chemists. 1995. Approved methods of the American Association of Cereal Chemists, 9th ed. American Association of Cereal Chemists, St. Paul, MN.
- Birch, L. C. 1945. The influence of temperature, humidity, and density on the oviposition of the small strain of *Calandra oryzae* L. and *Rhizopertha dominica* Fab. (Coleoptera). Aust. J. Exp. Biol. Med. Sci. 23: 197-203.
- Brader, B., R. C. Lee, R. Plarre, W. Burkholder, G. B. Kitto, C. Kao, L. Polston, E. Dorneanu, I. Szabo, B. Mead, B. Rouse, D. Sullins, and R. Denning. 2002. A comparison of screening methods for insect contamination in wheat. J. Stored Prod. Res. 38: 75-86.
- Chambers, J., N. J. McKevitt, and M. R. Stubbs. 1984. Nuclear magnetic resonance spectroscopy for studying the development and detection of the grain weevil, *Sitophilus granarius* (L.) (Coleoptera: Curculionidae), within wheat kernels. Bull. Entomol. Res. 74: 707-724.
- Dennis, N. M., and R. W. Decker. 1962. A method and machine for detecting living internal infestation in wheat. J. Econ. Entomol. 55: 199-203.
- Dowell, F. E., J. E. Throne, and J. E. Baker. 1998. Automated nondestructive detection of internal insect infestation of wheat kernels by using near-infrared reflectance spectroscopy. J. Econ. Entomol. 91: 899-904.
- [FDA] Food and Drug Administration. 1988. Wheat flour-adulterated with insect fragments and rodent hairs. Compliance Policy Guides, Chapter 4. Processed Grain Guide 7104.06. (http://www.fda.gov/ora/compliance_ref/cpg/cpgfod/cpg578-450.htm).
- Goosens, H. J. 1949. A method for staining insect egg plugs in wheat. Cereal Chem. 26: 419.
- [GIPSA] Grain Inspection, Packers and Stockyards Administration. 1993. Subpart M—United States standards for wheat. (<http://www.usda.gov/gipsa/reference-library/standards/810wheat.pdf>).
- Haff, R. P., and D. C. Slaughter. 2004. Real-time x-ray inspection of wheat for infestation by the granary weevil, *Sitophilus granarius* (L.). Trans. ASAE 47: 531-537.
- Harrison, R. D., W. A. Gardner, W. E. Tollner, and D. J. Kinard. 1993. X-ray computed tomography studies of the burrowing behavior of fourth-instar pecan weevil (Coleoptera: Curculionidae). J. Econ. Entomol. 86: 1714-1719.
- Johnson, S. N., D. B. Read, and P. J. Gregory. 2004. Tracking larval insect movement within soil using high resolution X-ray microtomography. Ecol. Entomol. 29: 117-122.
- Karunakaran, C., D. S. Jayas, and N.D.G. White. 2003a. Soft x-ray inspection of wheat kernels infested by *Sitophilus oryzae*. Trans. ASAE 46: 739-745.
- Karunakaran, C., D. S. Jayas, and N.D.G. White. 2003b. X-ray image analysis to detect infestations caused by insects in grain. Cereal Chem. 80: 553-557.
- Karunakaran, C., D. S. Jayas, and N.D.G. White. 2004. Detection of internal wheat seed infestation by *Rhizopertha dominica* using x-ray imaging. J. Stored Prod. Res. 40: 507-516.
- Neter, J., M. H. Kutner, C. J. Nachtsheim, and W. Wasserman. 1996. Applied linear regression models, 3rd ed. Irwin, Chicago, IL.
- Melvin, S. C., Karunakaran, D. S. Jayas, and N.D.G. White. 2003. Design and development of a grain singulation device. Can. Biosys. Eng. 45: 31-33.
- Mohsenin, N. N. 1984. Electromagnetic radiation properties of foods and agricultural products. Gordon and Breach Science Publishers, New York.
- Pearson, T. C., D. L. Brabec, and C. R. Schwartz. 2003. Automated detection of internal insect infestations in whole wheat kernels using a Perten SKCS 4100. Appl. Eng. Agric. 19: 727-733.
- Pedersen, J. R. 1992. Insects: identification, damage, and detection, pp. 435-489. In D. B. Sauer [ed.], Storage of cereal grains and their products, 4th ed. American Association of Cereal Chemists, St. Paul, MN.
- Perez-Mendoza, J., P. W. Flinn, J. F. Campbell, D. W. Hagstrum, and J. E. Throne. 2004. Detection of stored-grain insect infestation in wheat transported in railroad hopper-cars. J. Econ. Entomol. 97: 1474-1483.
- Perez-Mendoza, J., J. E. Throne, E. B. Maghirang, F. E. Dowell, and J. E. Baker. 2005. Insect fragments in flour: relationship to lesser grain borer (Coleoptera: Bostrichidae) infestation level in wheat and rapid detection using near-infrared spectroscopy. J. Econ. Entomol. 98: 2282-2291.
- Quinn, F.A.W. Burkholder, and G. B. Kitto. 1992. Immunological technique for measuring insect contamination of grain. J. Econ. Entomol. 85: 1463-1470.
- Ridgway, C., and J. Chambers. 1996. Detection of external and internal insect infestation in wheat by near-infrared reflectance spectroscopy. J. Sci. Food Agric. 71: 251-264.
- Schatzki, T. F., E. K. Wilson, G. B. Kitto, P. Behrens, and I. Heller. 1993. Determination of hidden *Sitophilus granarius* (Coleoptera: Curculionidae) in wheat by myosin ELISA. J. Econ. Entomol. 86: 1584-1589.
- Storey, C. L., D. B. Sauer, O. Ecker, and D. W. Fulk. 1982. Insect infestations in wheat and corn exported from the United States. J. Econ. Entomol. 75: 827-832.

- Throne, J. E.** 1994. Life history of immature maize weevils (Coleoptera: Curculionidae) on corn stored at constant temperatures and relative humidities in the laboratory. *Environ. Entomol.* 23: 1459–1471.
- Toews, M. D., and Bh. Subramanyam.** 2002. Sanitation in grain storage and handling, pp. 481–497. *In* Y. H. Hui [eds.], *Food plant sanitation*. Marcel Dekker, New York.
- Wehling, R. L., and D. L. Wetzel.** 1983. High-performance liquid chromatographic determination of low level uric acid in grains and cereal products as a measure of insect infestation. *J. Chromatogr.* 269: 191–197.
- Wehling, R. L., D. L. Wetzel, and J. R. Pedersen.** 1984. Stored wheat insect infestation related to uric acid as determined by liquid chromatography. *J. Assoc. Off. Anal. Chem.* 67: 644–647.
- White, G. D.** 1957. The practicality of flotation as a means for detecting infestation in wheat. *Down to Earth*, Summer. Dow Chemical Co., Midland, MI.

Received 8 July 2005; accepted 21 October 2005.
